FIGGIS, B. N. & REYNOLDS, P. A. (1987). *J. Chem. Soc. Dalton Trans.* pp. 1747–1753.
FIGGIS, B. N., REYNOLDS, P. A. & MASON, R. (1983). *J. Am. Chem. Soc.* **105**, 440–443.
FIGGIS, B. N., REYNOLDS, P. A. & WHITE, A. H. (1987). *J. Chem. Soc. Dalton Trans.* pp. 1737–1745.
FIGGIS, B. N., REYNOLDS, P. A. & WRIGHT, S. (1983). *J. Am. Chem. Soc.* **105**, 434–439.
KUNZE, K. L. & HALL, M. B. (1986). *J. Am. Chem. Soc.* **108**, 5122–5127.
MCEACHRAN, R. P., STAUFFER, A. D. & GREITA, S. (1979). *J. Phys. B*, **12**, 3119–3123.
MAHAN, G. D. (1980*a*). *Chem. Phys. Lett.* **76**, 183–185.
MAHAN, G. D. (1980*b*). *Phys. Rev. A*, **22**, 1780–1785.
SEILER, P. & DUNITZ, J. D. (1986). *Helv. Chim. Acta*, **69**, 1107–1112.
VAN STAPELE, R. P., BELJERS, H. G., BONGERS, P. F. & ZIJLSTRA, H. (1966). *J. Chem. Phys.* **44**, 3719–3715.
WILLIAMS, G. A., FIGGIS, B. N. & MASON, R. (1981). *J. Chem. Soc. Dalton Trans.* pp. 734–742.

Acta Cryst. (1989). B**45**, 247–251

Structure Refinements of Lead-Substituted Calcium Hydroxyapatite by X-ray Powder Fitting

BY A. BIGI AND A. RIPAMONTI

Dipartimento di Chimica 'G. Ciamician', Universita' degli Studi, Via Selmi 2, *I*-40126 *Bologna, Italy*

AND S. BRÜCKNER

Dipartimento di Chimica, Politecnico, Piazza Leonardo da Vinci 32, *I*-20133 *Milano, Italy*

AND M. GAZZANO AND N. ROVERI

Centro di Studio per la Fisica delle Macromolecole (CNR), c/o Dipartimento di Chimica, Universita' degli Studi, Via Selmi 2, *I*-40126 *Bologna, Italy*

AND S. A. THOMAS

Department of Chemistry, Ahmadu Bello University, Zaria, Nigeria

(*Received* 22 *August* 1988; *accepted* 6 *February* 1989)

Abstract

The crystal structures of hydroxyapatites, synthesized at different degrees of lead substitution for calcium (20, 45 and 80% Pb atoms) by solid-state reaction at 1173 K, have been investigated by X-ray powder-pattern fitting. The disagreement factors (R_{wp}) are 5·9, 6·0 and 6·6% for Pb20, Pb45 and Pb80, respectively. The site-occupancy factors of Pb atoms indicate a clear preference of lead for site (2) of the apatite structure, which may be responsible for the observed deviations of the *c*-axis dimension from Vegard's law. An increasing shift of the OH group above or below the center of the Pb(2) triangles has been observed with increasing lead content. The JCPDS file Nos. for Pb20, Pb45 and Pb80 are 40-1497, 40-1496 and 40-1495, respectively.

Introduction

The structure of hydroxyapatite (HA) can easily accommodate a great variety of substituents, both anionic and cationic (Lang, 1981; LeGeros & LeGeros, 1984). Among the cations which can be incorporated in the HA structure, only cadmium, strontium and lead are known to replace calcium over the whole range of composition. The *a*- and *c*-axis dimensions of both strontium–calcium apatites and cadmium–calcium apatites vary linearly with composition according to Vegard's law (Heijligers, Driessens & Verbeeck, 1979; Bigi, Gazzano, Ripamonti, Foresti & Roveri, 1986). Lead can substitute for calcium in the HA structure over the whole range of composition causing an enlargement of the unit cell. Although in earlier papers (Muller, 1947; Narasaraju, Singh & Rao, 1972; Rao, 1976) the lattice parameters of lead–calcium hydroxyapatite were reported to vary linearly with the composition, more recently deviations of the *c* parameter from Vegard's law have been observed (Engel, Krieg & Reif, 1975; Verbeeck, Lassuyt, Heijligers, Driessens & Vrolijk, 1981; Andres-Verges, Higes-Rolando, Valenzuela-Calahorro & Gonzalez-Diaz, 1983). The observed deviations from Vegard's law have been attributed to a possible preference of the Pb^{2+} ion for site (2) of the apatite structure, on the basis of the cation distribution deduced from the relative intensities of suitable reflections in the powder diffractogram

0108-7681/89/030247-05$03.00

(Engel *et al.*, 1975; Andres-Verges *et al.*, 1983). Furthermore, the structure analysis of a sample of $Pb_9(PO_4)_6$ prepared by hydrothermal reaction (Hata, Marumo, Iwai & Aoki, 1980) revealed a deficiency of lead in site (1). In contrast, the results of structure refinements of lead–calcium hydroxyapatite solid solutions by an X-ray powder-pattern-fitting method led to a suggestion of random distribution of lead in sites (1) and (2) (Miyake, Suzuki & Ishigaki, 1986).

In order to determine the possible site preference of Pb atoms in hydroxyapatite we have refined the crystal structures of hydroxyapatite samples containing 20% (Pb20), 45% (Pb45) and 80% (Pb80) Pb atoms by an X-ray powder-pattern-fitting method (Rietveld method). The results indicate a clear preference of lead ions for site (2) of the apatite structure, which can be responsible for the observed deviations of the *c*-axis dimension from Vegard's law.

Experimental

Lead–calcium hydroxyapatite solid solutions were obtained by solid-state reaction of appropriate mixtures of lead apatite and calcium apatite at 1173 K overnight. Calcium and lead apatites were previously prepared by reaction of $Ca(OH)_2$ and $Pb_6O_5(NO_3)_2$ respectively, with H_3PO_4. Details of the method of synthesis are reported in a separate paper (manuscript in preparation).

The structure refinements were carried out on samples containing 20, 45 and 80% Pb atoms. A very small amount of PbO (JCPDS file No. 5-0570) was detected in the X-ray patterns of the samples containing 20 and 80% Pb atoms. Powder X-ray diffraction analysis was carried out with a Philips PW1050/81 diffractometer controlled by a PW 1710 unit. The diffractometer was equipped with Soller slits and proportional detector PW 1711/10. The area of the sample holder was 14 × 20 mm and no automatic divergence slits were used. The data were processed on an Olivetti M24 computer. The experimental details of data collection are reported in Table 1 and a summary of the powder data is given in Table 2.

2400 intensity values were collected for each sample, and the number of refined parameters are 26, 24 and 25 for Pb20, Pb45 and Pb80, respectively. The $(\Delta/\sigma)_{max}$ values for Pb20, Pb45 and Pb80 are 0·91, 0·83 and 0·94, respectively.

Structural analysis

The Pb45 structure was refined first, starting from the fractional coordinates of pure hydroxyapatite (Kay & Young, 1964) and allowing for an equiprobable substitution by Pb atoms at sites (1) and (2). The refinement routine is substantially that of Immirzi (1980) modified by one of the authors of the present communication (SB), for peak asymmetry and its dependence on 2θ.

Table 1. *Experimental details of X-ray powder-profile data collection*

Radiation	Cu $K\alpha$, Ni-filtered (45 kV, 30 mA)
Divergence slit	0·5°
Receiving slit	0·1 mm
Scattering slit	0·5°
Step width	0·03° (2θ)
Count time	30 s each step
2θ range	8–80° (2θ)
Temperature	Room temperature

Table 2. *A summary of the powder data*

Pb20			Pb45			Pb80		
2θ	*hkl*	I/I_o*	2θ	*hkl*	I/I_o*	2θ	*hkl*	I/I_o*
10·76	0 1 0	4	10·63	0 1 0	15	10·46	0 1 0	1
16·70	0 1 1	1	16·44	0 1 1	0·5	16·01	0 1 1	0
18·70	1 1 0	5	18·47	1 1 0	6	18·16	1 1 0	0·5
21·62	0 2 0	10	21·35	0 2 0	9	21·00	0 2 0	16
22·69	1 1 1	9	22·36	1 1 1	29	21·87	1 1 1	24
25·62	0 0 2	22	25·17	0 0 2	27	24·32	0 0 2	9
27·86	0 1 2	10	27·39	0 1 2	14	26·53	0 1 2	16
28·74	2 1 0, 1 2 0	24	28·37	2 1 0, 1 2 0	19	27·90	2 1 0, 1 2 0	21
31·54	2 1 1, 1 2 1	100	31·12	2 1 1, 1 2 1	100	30·51	2 1 1, 1 2 1, 1 1 2	100
31·91	1 1 2	20	31·40	1 1 2	21			
32·68	0 3 0	30	32·27	0 3 0	15	31·73	0 3 0	20
33·77	0 2 2	1	33·24	0 2 2	0	32·34	0 2 2	0
37·92	2 2 0	0·5	37·44	2 2 0	1	36·80	2 2 0	0
38·88	1 2 2, 2 1 2	3	38·29	1 2 2, 2 1 2	7	37·34	1 2 2, 2 1 2	2
39·53	1 3 0, 3 1 0	11	39·02	1 3 0, 3 1 0	5	38·36	1 3 0, 3 1 0	1·5
40·15	2 2 1	2	39·62	2 2 1	1·5	38·87	2 2 1	0·5
43·45	1 1 3	7	42·70	1 1 3	12	41·36	1 1 3	8
44·07	0 4 0	7	43·50	0 4 0	9	42·76	0 4 0, 0 2 3	5
46·33	2 2 2	13	45·64	2 2 2	10	44·60	2 2 2	15
47·70	3 1 2, 1 3 2	9	47·00	3 1 2, 1 3 2	8	45·94	3 1 2, 1 3 2	9
48·26	3 2 0, 2 3 0	4	47·63	3 2 0, 2 3 0	3	46·81	3 2 0, 2 3 0, 2 1 3, 1 2 3	22
49·04	2 1 3, 1 2 3	24	48·22	2 1 3, 1 2 3	28			
50·12	3 2 1, 2 3 1	16	49·45	3 2 1, 2 3 1	17	48·52	3 2 1, 2 3 1	13
50·91	4 1 0, 1 4 0	11	50·24	4 1 0, 1 4 0	8	49·36	4 1 0, 1 4 0	11
51·67	0 4 2	14	50·92	0 4 2	18	49·81	0 4 2, 0 0 4	22
52·65	0 0 4	6	51·66	0 0 4	7			

* Intensities were simply estimated from the maximum peak heights above background.

Peak shapes were described through Pearson VII distributions (Hall, Veeraraghavan, Rubin & Whinchell, 1977) while half-height widths as a function of 2θ were described through the expression

$$H_k^2 = U\tan^2 2\theta_k + V\tan 2\theta_k + W.$$

Remarkable asymmetry affects peak shapes at low 2θ values, becoming less and less evident at increasing diffraction angles. This effect, due to the instrumental setting, was taken into account by building up the whole peak shape through the juxtaposition of two half peaks each one being characterized by its own half-height width, H'_k and H''_k, while the overall subtended area was kept equal to the calculated peak intensity. The 2θ dependence of this effect was taken into account by

Table 3. *Refined non-structural parameters for the three structures*

	Pb20	Pb45	Pb80
Zero correction 2θ (°)	−0·0512 (6)	−0·0456 (3)	−0·0577 (5)
Profile function parameters*			
U	0·76 (6)	0·34 (2)	0·62 (6)
V	−0·17 (4)	−0·09 (1)	−0·12 (4)
W	0·046 (6)	0·031 (2)	0·033 (6)
m	1·80 (5)	1·92 (4)	1·62 (3)
Preferred orientation parameter†	−0·211 (5)	0	−0·028 (6)
Background intensities (k counts) at nodes of the segmented line			
2θ(°) = 8·0	0·369 (5)	0·276 (4)	0·573 (9)
10·0	0·388 (4)	0·303 (3)	0·627 (6)
12·0	0·359 (2)	0·229 (2)	—
14·0	—	—	0·508 (3)
20·0	0·383 (2)	0·197 (1)	—
34·0	0·394 (3)	0·185 (1)	0·510 (3)
40·0	0·308 (3)	0·156 (1)	0·461 (3)
45·0	0·338 (2)	—	—
52·0	—	—	0·482 (3)
55·0	0·302 (2)	—	—
64·0	—	—	0·439 (3)
80·0	0·262 (2)	0·127 (1)	0·455 (3)
Asymmetry parameter‡	0	38·7 (4)	0
Cell dimensions (Å)			
a	9·491 (2)	9·609 (2)	9·769 (2)
c	6·953 (2)	7·077 (2)	7·320 (2)

* According to the relation $H_k^2 = U\tan^2\theta_k + V\tan\theta_k + W$; m is the exponent in the Pearson VII profile function $f(z) = (C/H_k)[1 + 4(2^{1/m}-1)\,z^2]^{-m}$ with $z = (2\theta_i - 2\theta_k)/H_k$.

† Preferred orientation factor PO = $\exp(-G\alpha_k^2)$, α_k is the angle between the scattering vector of the kth reflection and the scattering vector of a fixed (preferred) orientation, in this case the 002 reflection. In the case of Pb45 we found no evidence for a preferred orientation effect.

‡ See text for a description of the present approach to peak asymmetry. In Pb20 and Pb80 spectra this effect was not detected.

Table 4. *Refined structural parameters for the three structures*

	x	y	z	OF*	B (Å^2)
Pb20 (21·5)†					
Ca(1), Pb(1)	0·3333	0·6667	0·0058 (25)	0·0115 (9)	1·4
Ca(2), Pb(2)	0·2399 (5)	0·9943 (7)	0·25	0·1696 (22)	2·0
P	0·4074 (8)	0·3727 (7)	0·25	0·5	1·0
O(1)	0·3497 (16)	0·4985 (13)	0·25	0·5	2·0
O(2)	0·5948 (8)	0·4581 (14)	0·25	0·5	2·0
O(3)	0·3425 (10)	0·2670 (7)	0·0673	1·0	2·0
O(h)	0·0	0·0	0·1897 (50)	0·167	2·0
Pb45 (45·2)†					
Ca(1), Pb(1)	0·3333	0·6667	0·0099 (20)	0·0216 (8)	1·4
Ca(2), Pb(2)	0·2417 (3)	0·9984 (5)	0·25	0·3552 (24)	2·0
P	0·4126 (7)	0·3784 (6)	0·25	0·5	1·0
O(1)	0·3558 (14)	0·5029 (11)	0·25	0·5	2·0
O(2)	0·5977 (7)	0·4626 (13)	0·25	0·5	2·0
O(3)	0·3484 (9)	0·2741 (6)	0·0705	1·0	2·0
O(h)	0·0	0·0	0·1515 (32)	0·167	2·0
Pb80 (83·9)†					
Ca(1), Pb(1)	0·3333	0·6667	0·0066 (20)	0·2121 (40)	1·4
Ca(2), Pb(2)	0·2437 (5)	0·9982 (10)	0·25	0·4869 (60)	2·0
P	0·4092 (16)	0·3706 (11)	0·25	0·5	1·0
O(1)	0·3464 (29)	0·4874 (23)	0·25	0·5	2·0
O(2)	0·5916 (16)	0·4599 (25)	0·25	0·5	2·0
O(3)	0·3495 (20)	0·2675 (11)	0·0765	1·0	2·0
O(h)	0·0	0·0	0·0120 (88)	0·167	2·0

* The occupation factors reported refer to Pb atoms. The corresponding values for Ca atoms can be obtained as a difference from 0·3333 for site (1) and from 0·5 for site (2).

† Overall lead content (%) calculated from the occupancy factors.

assuming the difference $H'_k - H''_k$ changes as $A/(2\theta)^2$ where A is an adjustable parameter. This is, of course, an empirical approach whose validity is only supported by the substantial improvement in the best-fit results.

Table 5. Ca—Ca *distances* (Å) *and displacements* (Å) *of the* P *atoms from the origin*

	HA	Pb20	Pb45	Pb80
(*a*) Ca—Ca distances				
Ca(1)—Ca(1)	3·422 (2)	3·396 (30)	3·398 (27)	3·563 (28)
Ca(2)—Ca(2)	4·081 (2)	3·994 (9)	4·036 (8)	4·139 (12)
(*b*) P-atom displacement*				
ΔX	2·019 (4)	2·094 (12)	2·149 (13)	2·183 (14)
ΔY	3·008 (4)	3·061 (8)	3·149 (8)	3·133 (9)
φ (°)	30·8 (2)	27·1 (4)	27·0 (3)	29·3 (4)

* The P-atom displacements from the origin are expressed in an orthogonal reference frame (see text). The orientation of the phosphate moiety is described in terms of the angle φ between the P—O(2) bond and the X axis.

The background line was approximated by a segmented line where only the height of the nodes was refined while their position on the 2θ scale was arbitrarily fixed. The height of the background nodes was allowed to vary during the whole refinement procedure.

The first refinement cycles immediately showed a marked prevalence of lead in site (2).

In the final cycles the phosphate moiety was adjusted as a rigid body in a cell; one torsion angle around an axis passing through phosphorus and parallel to c, and two translations along a and b were the corresponding refinable parameters. No attempt was made to distinguish the location of Ca atoms from that of the substituting Pb atoms. Thermal factors were not refined: only at the end of the refinement procedure and after a few trials were those of Pb(1)[Ca(1)], Pb(2)[Ca(2)] and P slightly changed to obtain a better overall agreement with observed data; these changes in the thermal factors do not significantly affect the occupation factors. No constraint was imposed on the overall lead content but only the condition of complementarity of the occupation factors of Ca(1) and Ca(2) with those of Pb(1) and Pb(2), respectively. The resulting overall lead content [45·2(3)%] is in good agreement with the analytical data and, in view of the unconstrained procedure adopted in its evaluation, is also an indication that the choice of the thermal factors is in the correct range. Good agreement between analytical data and refined occupation factors was also found for Pb20 and Pb80 (see Table 4).

The Pb20 and Pb80 structure refinements proceeded substantially along the same lines as that of Pb45, the most significant difference being the presence of PbO traces. This presence is responsible for a slight worsening of the computed disagreement factors but is not expected to have any influence on the refinement procedure since the most intense peaks of PbO do not overlap significantly with the peaks of interest in the present analysis. The overall calculated lead contents of the Pb20 and Pb80 samples are 21·5 (5) and 83·9 (9)%, respectively.

Refined non-structural parameters for the three structures are reported in Table 3.

In Figs. 1, 2 and 3 we compare the observed [curve (*a*)] and calculated [curve (*b*)] powder diffraction patterns of Pb20, Pb45 and Pb80, respectively. The (*c*) curves show the difference profiles and the dotted lines

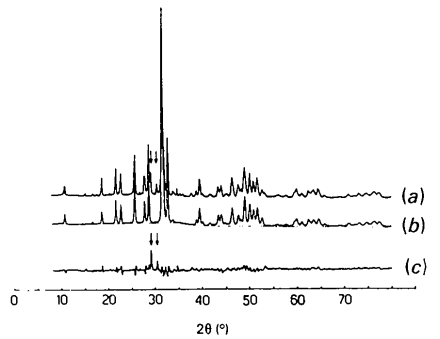

Fig. 1. A comparison of the observed [curve (*a*)] and calculated [curve (*b*)] powder diffraction patterns of Pb20. Curve (*c*) is the difference profile. The dashed line is the calculated background contribution; the arrows indicate the reflections due to the PbO phase (see text).

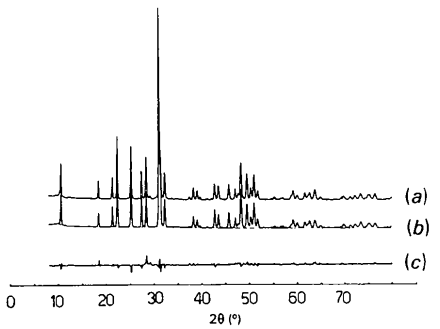

Fig. 2. A comparison of the observed [curve (*a*)] and calculated [curve (*b*)] powder diffraction patterns of Pb45. Curve (*c*) is the difference profile. The dashed line is the calculated background contribution.

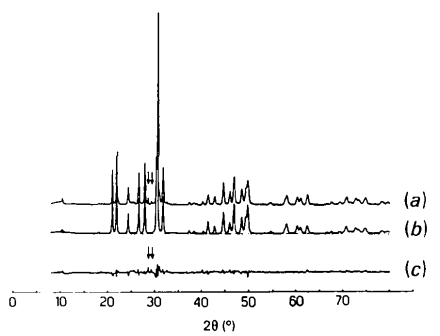

Fig. 3. A comparison of the observed [curve (*a*)] and calculated [curve (*b*)] powder diffraction patterns of Pb80. Curve (*c*) is the difference profile. The dashed line is the calculated background contribution; the arrows indicate the reflections due to the PbO phase (see text).

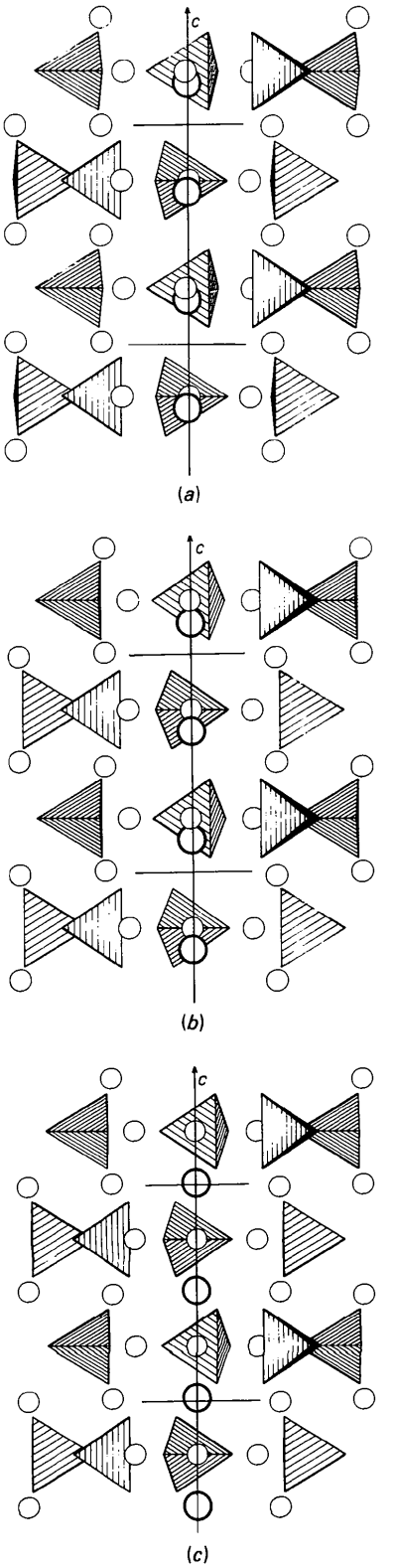

Fig. 4. A view along [010] direction for: (*a*) HA, (*b*) Pb45 and (*c*) Pb80. O(*h*) is represented by thick circles. (Plot program: Fischer, 1985.)

represent the background contributions. The disagreement factors, in the form of

$$R_{wp} = \left\{ \frac{\sum w_i[y_i(\text{obs}) - y_i(\text{calc})]^2}{\sum w_i[y_i(\text{obs})]^2} \right\}^{1/2}$$

are 7·7, 6·0 and 6·6% for Pb20, Pb45 and Pb80, respectively. The disagreement factor of 7·7% for Pb20 drops to 5·9% when contributions from the PbO phase are ignored. In Table 4 the refined fractional coordinates, occupation factors and thermal factors for the three structures are reported. Table 5 describes the effect of an increasing lead content upon (*a*) the Ca–Ca distances and (*b*) the location of the phosphate moiety in the cell. For each structure we report the displacements (Å) of the P atoms from the origin, expressed in an orthogonal reference frame with *x* and *z* coincident with *a* and *b*, and *y* defining a right-handed system. The orientation of the molecules is defined through the angle between the P–O(1) bond and the *x* axis.

Discussion

The hexagonal unit cell of hydroxyapatite contains ten cations arranged on two non-equivalent sites; four on site (1) and six on site (2). Calcium ions in site (1) occur aligned in columns and those in site (2) in equilateral triangles centered on the screw axes. Calcium ions in site (1) are surrounded by three O(1), three O(2) and three O(3) oxygen atoms, whereas one O(*h*), one O(1), one O(2) and four O(3) atoms surround calcium ions in site (2).

The results of the powder-fitting structure refinements indicate a clear preference of lead ions for site (2) of the apatite structure. When lead substitutes for calcium in the apatite structure, it fills almost exclusively site (2), until, at Pb-atom contents higher than 45%, it also begins to fill site (1) significantly. In fact, the occupancy factors of Pb^{2+} ions on site (2) are 20·1, 42·6 and 58·4% for Pb20, Pb45 and Pb80, respectively. This result can account for the discontinuity, at about 50–60% Pb atoms, in the curve of the *c*-axis dimension against lead content (Engel *et al.*, 1975; Andres-Verges *et al.*, 1983). The substitution of lead for calcium in the columns parallel to the *c* axis [site (1)], provokes a greater enlargement of the *c*-axis dimension than that induced by lead substitution in site (2). In HA and in lead-substituted samples the Ca(2)–Ca(2) distances are larger than the Ca(1)–Ca(1) distances, therefore the former do not change appreciably up to a lead content of about 45%, while the latter are strongly affected even when a little amount of the larger ion is present, as can be seen from the data reported in Table 5(*a*).

Lead incorporation in the apatite structure causes small displacements of the P atoms from the origin of the unit cell (see Table 5*b*) but affects significantly the position of the OH group which shifts above or below the center of the Pb(2) triangles as shown in Fig. 4, where the increase in shift as a function of lead content can be appreciated. This shift is more evident at lead contents higher than 45%, that is when lead is present in high percentage in site (2), and induces an increase in the coordination number of Pb(2).

The authors are grateful to Consiglio Nazionale delle Ricerche and Ministero della Pubblica Istruzione, Italy, for financial support. One of the authors (SAT) has carried out this work with the support of the 'TWAS Italian Awards Scheme for Research and Training in Italian Laboratories'.

References

ANDRES-VERGES, M., HIGES-ROLANDO, F. J., VALENZUELA-CALAHORRO, C. & GONZALEZ-DIAZ, P. F. (1983). *Spectrochim. Acta*, **39A**, 1077–1082.

BIGI, A., GAZZANO, M., RIPAMONTI, A., FORESTI, E. & ROVERI, N. (1986). *J. Chem. Soc. Dalton Trans.* pp. 241–244.

ENGEL, G., KRIEG, F. & REIF, G. (1975). *J. Solid State Chem.* **15**, 117–126.

FISCHER, R. X. (1985). *J. Appl. Cryst.* **18**, 258–262.

HALL, M. M. JR, VEERARAGHAVAN, V. G., RUBIN, H. & WHINCHELL, P. G. (1977). *J. Appl. Cryst.* **10**, 66–68.

HATA, M., MARUMO, F., IWAI, S. & AOKI, H. (1980). *Acta Cryst.* B**36**, 2128–2130.

HEIJLIGERS, H. J. M., DRIESSENS, F. C. M. & VERBEECK, R. M. H. (1979). *Calcif. Tissue Int.* **29**, 127–131.

KAY, M. I. & YOUNG, R. A. (1964). *Nature (London)*, **204**, 1050–1052.

IMMIRZI, A. (1980). *Acta Cryst.* B**36**, 2378–2385.

LANG, J. (1981). *Bull. Soc. Sci. Bretagne*, **53**, 95–124.

LEGEROS, R. Z. & LEGEROS, J. P. (1984). *Phosphate Minerals*, edited by J. O. NIRIDGN & P. B. MOORE, pp. 351–385. New York: Springer.

MIYAKE, M., SUZUKI, T. & ISHIGAKI, K. (1986). *J. Solid State Chem.* **61**, 230–235.

MULLER, M. (1947). *Helv. Chim. Acta*, **30**, 2069–2080.

NARASARAJU, T. S. B., SINGH, R. P. & RAO, V. L. N. (1972). *J. Inorg. Nucl. Chem.* **34**, 2072–2074.

RAO, S. V. C. (1976). *J. Indian Chem. Soc.* **53**, 352–354.

VERBEECK, R. M. H., LASSUYT, C. J., HEIJLIGERS, H. J. M., DRIESSENS, F. C. M. & VROLIJK, J. W. G. A. (1981). *Calcif. Tissue Int.* **33**, 243–247.